Monte Carlo Tree Search for 3D/2D Registration of Vessel Graphs

Jianjun Zhu
School of Optics and Photonics
Beijing Institute of Technology
Beijing, China
jjzhubit@163.com

Shuang Song
School of Optics and Photonics
Beijing Institute of Technology
Beijing, China
ssbit_2013@163.com

Shuai Guo
School of Optics and Photonics
Beijing Institute of Technology
Beijing, China
1036435458@qq.com

Danni Ai
School of Optics and Photonics
Beijing Institute of Technology
Beijing, China
danni@bit.edu.cn

Jingfan Fan
School of Optics and Photonics
Beijing Institute of Technology
Beijing, China
fjf@ bit.edu.cn

Hong Song
School of Computer Science & Technology
Beijing Institute of Technology
Beijing, China
anniesun@bit.edu.cn

Ping Liang
Department of Interventional Ultrasound
Chinese PLA General Hospital
Beijing, China
liangping301@126.com

Jian Yang*
School of Optics and Photonics
Beijing Institute of Technology
Beijing, China
jyang@bit.edu.cn

***Abstract*—3D/2D registration techniques can compensate for the deficiencies of X-ray angiography-based navigation in vascular interventional surgery, such as the lack of depth information and excessive use of contrast agents. In this study, we propose a novel Monte Carlo tree search-based 3D/2D vessel graph registration method. The registration problem is transferred to a tree search problem according to the topology of vessel centerlines. Then, the Monte Carlo tree search method is applied to find the optimal vessel matching associated with highest registration score. Experiments on uninitialized vessel data demonstrate that the proposed method can achieve the highest accuracy among four state-of-the-art methods. An average accuracy of 1.91 mm on clinical coronary artery data is obtained. For the independence of initial pose and robustness to noise, the proposed method can align 3D and 2D vessels without prior initialization in vascular interventional surgery.**

Key words—3D/2D Registration, Vessel Graph Matching, Monte Carlo Tree Search

I. INTRODUCTION

X-ray angiography (XRA) is the current primary guide for minimally invasive vascular interventions. In such interventions, emitted X-rays penetrate and project the tissues on the image plane to display the vascular lumen after injecting contrast agents into the arteries of interest through a catheter. Although XRA has high spatial and temporal resolution, it lacks spatial depth information, and the excessive use of contrast agents increases the burden on patients. 3D/2D registration can be used to fuse the projection of 3D vessels extracted from preoperative computed tomography angiography (CTA) images with XRA, which can provide depth information of vessels for the interventional radiologists and provide certain support for the operation of the instrument under images with low or no contrast agents.

For feature-based registration methods, cross-dimensional features are required. For vascular structures, the centerlines extracted from CTA and XRA inherently contain anatomical structure correspondences. Thus, they are the most commonly used feature in current vascular registration methods [1]. Point set registration (PSR) is a process of determining spatial transformation that aligns two point sets [2]. All state-of-the-art feature-based 3D/2D registration methods are the extensions of classical PSR methods. The iterative closest point (ICP) method [3] alternately estimates correspondences and transformations, in which the correspondences are assigned by the nearest neighbor relation, and the transformation is obtained by a closed-form solution. An extension of ICP for 3D/2D registration is achieved by back-projecting 2D points onto a 3D space and performing general ICP [4]. Rivest-Hénault et al. [5] designed an objective function using a precomputed distance transform of the 2D vessel centerline, thereby accelerating the ICP registration process. Benseghir et al. [6] proposed the iterative closest curve method, which uses the nearest neighbor relation of the vascular segment curve instead of points to construct the objective function. These ICP-like 3D/2D registration methods also have the drawbacks of classical ICP methods, such as sensitivity to noise and outliers and dependence on initial pose.

Soft assignment-based methods have been proposed to address the problem on noise and outliers. Myronenko et al. [7] redefined the point set registration problem with the EM framework. In expectation-step, the Gaussian mixture model (GMM) is used to assign the correspondence probability of the point set. In maximization-step, a closed-form solution is used to calculate the transformation. For the nonlinear nature of 3D/2D registration, the closed-form solution of transformation cannot be derived. Thus, Kang et al. [8] utilized particle swarm optimization to conduct global searching instead of the closed-form solution. Jian et al. [9] regarded the similarity measures of point set registration as an L_2 distance of two Gaussian mixture responses and calculated the L_2 distance using the reproducing property of inner product of kernel function. Baka et al. [4] extended [9] to 3D/2D registration and proposed the oriented GMM (OGMM) method, which encodes the orientation information of vessels into the L_2 distance to achieve accurate registration results.

For the problem of initial pose dependence, these methods, which construct objective function and then refine it via

978-1-7281-1867-3/19/$31.00 ©2019 IEEE

numerical optimization, cannot solve it effectively. In 3D/2D registration, CTA and DSA data are collected from different devices, and a pose difference usually exists between them. Some initialization approaches, such as the alignment of patient position and orientation, the registration of corresponding pairs of markers, and manual initialization, were introduced in [1]. However, an automatic initialization method that uses intrinsic features is more suitable for intraoperative 3D/2D registration. To obtain pose independence, the registration based on a match-then-transform framework is more appropriate than optimization-based methods [10, 11].

With vessel topology as an invariant property across modalities and dimensions, graph matching has become an effective vascular 3D/2D registration approach. Vessel graph matching has been described as the process of estimating the correspondences of vessel bifurcations and then matching vessel curves between paired bifurcations by considering them as vertices. Serradell et al. [12] treated vessel registration as a search process for most likely correspondences and conducted a priority search to accelerate the process. Pinheiro et al. [13] formulated vessel matching as a tree-searching method based on the topology consistency of two graphs for matching. The Monte Carlo tree search was then applied to solve this problem. The above-mentioned methods are associated with 3D/3D or 2D/2D vasculature matching/registration.

In this study, we extend the work [13] to 3D/2D vessel registration and refer the proposed method as *Monte Carlo tree search for 3D/2D registration* (MCTSR). According to the property that the vessel matching can be decomposed into continuous correlated states based on vascular topology, these states can be constructed as a tree. Using the dense correspondences of 3D and 2D vessel points and the closed-form solution of perspective-*n*-points (P*n*P) problem [14], the mapping of vessel matching to transformation can be established. In addition, the evaluation score of 3D/2D registration can be estimated based on the transformation. Therefore, the current 3D/2D vessel matching state, as well as the corresponding registration result and evaluation score are recorded at each node of the search tree. The Monte Carlo tree search (MCTS) [15] strategy is used to find the optimal vessel matching state associated with the highest score. We demonstrate the effectiveness of the proposed method on clinical coronary arteries and aortic model data. The main contributions of this study are to transform the 3D/2D vessel registration task into the problem of finding the best match through the search tree based on the topological information of blood vessels, and obtain the accurate registration results by using the MCTS strategy.

II. Methods

The purpose of 3D/2D registration is to find the optimal spatial transformation that transforms the 3D vessels into the target space of XRA acquisition equipment. Then, the 3D vessels can be projected onto a 2D plane according to the imaging parameters of XRA and overlap the 2D vessels.

2.1 Problem Definition

Vessel topology can be formulated as $\mathcal{G} = \{\mathcal{V}, \mathcal{E}\}$, where $\mathcal{V}$ denotes the vertex set containing vascular endpoint and bifurcations, $\mathcal{E} \subseteq \mathcal{V} \times \mathcal{V}$ denotes the edge set of the vessel branch curve connecting two adjacent vertices. The 3D and 2D vessel graphs are formulated as $\mathcal{G}^{\mathrm{A}} = \{\mathcal{V}^{\mathrm{A}}, \mathcal{E}^{\mathrm{A}}\}$ and $\mathcal{G}^{\mathrm{B}} = \{\mathcal{V}^{\mathrm{B}}, \mathcal{E}^{\mathrm{B}}\}$. Registration of the 3D and 2D vessel structure can be formulated as finding an optimal transformation T of the 3D vessel, whose projection best aligns the 2D vessel,

$$\hat{T} = \underset{T \in \Omega_T}{\operatorname{argmin}}\, \mathcal{D}(P \circ T(\mathcal{G}^{\mathrm{A}}), \mathcal{G}^{\mathrm{B}}), \tag{1}$$

where $\mathcal{D}$ quantifies the distance between two registered vessel graphs, P denotes perspective projection operation that is constant and mandatory to register 3D and 2D modality, it can be established using several parameters obtained from the DICOM head file of XRA. T denotes 3D rigid transformation, Ω_T is the domain of admissible transformation.

The dense correspondence between 3D point set $\mathbf{C}^{\mathrm{A}} \in \mathbb{R}^{|\mathbf{C}^{\mathrm{A}}|\times 3}$ and 2D point set $\mathbf{C}^{\mathrm{B}} \in \mathbb{R}^{|\mathbf{C}^{\mathrm{B}}|\times 2}$ can be expressed as $\pi = \{(\boldsymbol{c}_i^{\mathrm{A}}, \boldsymbol{c}_j^{\mathrm{B}})\}$. Given that π is obtained, the goal of registration is similar to the P*n*P problem in the computer vision area. It aims to determine the camera pose by reducing the problem of estimating the transformation of the paired points to estimating coordinates of four control points. A closed-form solution REPP*n*P [14] is applied here to solve the P*n*P problem, in which the outlier correspondences are rejected by the low-rank restriction of homogeneous system. Thus, a surjection $f_1: \pi \in \Omega_\pi \to T \in \Omega_T$ from the dense matching π to transformation T can be obtained, where Ω_π denotes the solution domain of π. Therefore, the registration problem can be transferred into that of solving the dense matching of 3D and 2D vessel points.

In this study, a 3D vessel is considered an acyclic graph. A 2D vessel is generally represented by a cyclic 2D graph because several projected 3D branches overlap in the 2D plane, thus forming fake bifurcations and connecting edges. Thus, 3D and 2D vascular topologies are usually inconsistent $\mathcal{G}^{\mathrm{A}} \neq \mathcal{G}^{\mathrm{B}}$. The goal of vessel matching is to find the maximal topological consistency of $\mathcal{G}^{\mathrm{A}}$ and $\mathcal{G}^{\mathrm{B}}$, similar to the subgraph isomorphism problem. The matching of vertex and edges in isomorphic subgraphs $\acute{\mathcal{G}}^{\mathrm{A}} \subseteq \mathcal{G}^{\mathrm{A}}$ and $\acute{\mathcal{G}}^{\mathrm{B}} \subseteq \mathcal{G}^{\mathrm{B}}$ can be expressed as $\pi^{\mathcal{V}} = \{(v_i^{\mathrm{A}}, v_j^{\mathrm{B}})\}$ and $\pi^{\mathcal{E}} = \{(e_i^{\mathrm{A}}, e_j^{\mathrm{B}})\}$. Since the end-vertices of matched edges are matched and no other vertices are involved, the edge matching $\pi^{\mathcal{E}}$ uniquely determines a vertex matching $\pi^{\mathcal{V}}$. The dense matching π of two vessel graphs is addressed by starting to make sparse correspondences between vertices and then aligning edges between paired vertices by considering them as anchor points. In this study, the dense correspondence of edges can be estimated using a uniform interpolation. Then, a surjection $f_2: \pi^{\mathcal{E}} \in \Omega_{\pi^{\mathcal{E}}} \to \pi \in \Omega_\pi$ from $\pi^{\mathcal{E}}$ to π can be obtained, where $\Omega_{\pi^{\mathcal{E}}}$ is associated with the solution domain of $\pi^{\mathcal{E}}$. The problem of vessel registration can be further transferred into matching of graph edges.

2.2 Monte Carlo Tree Search

Based on the definition of $\pi^{\mathcal{E}}$ and topological continuity, we can gradually increase the matching edges along the

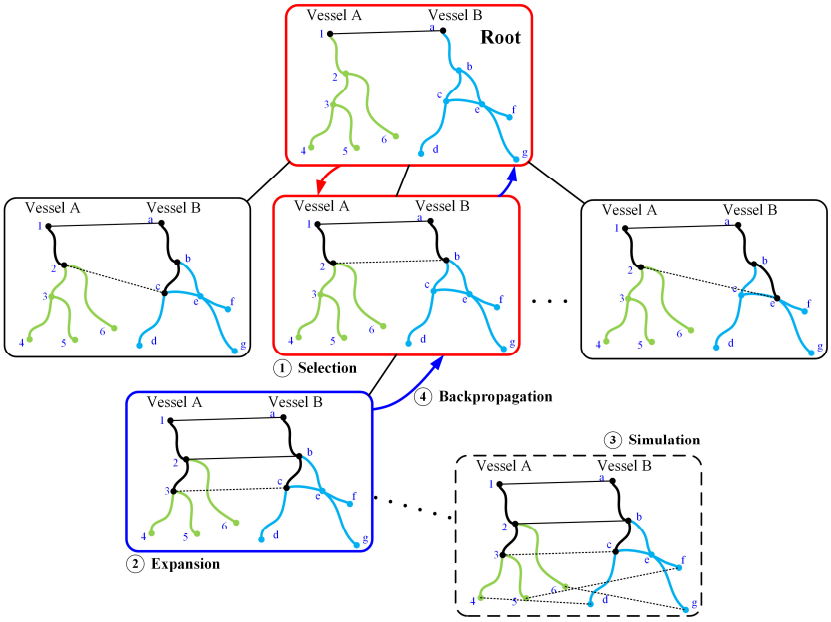

Fig. 1. One iteration of the MCTSR procedure for matching a pair of vessel graphs. A pair of vessel vertices is selected at root node, then the tree is extended through four steps, including selection, expansion, simulation and backpropagation.

vascular graph when the initial matched vertex pair $\pi^{\mathcal{E}}_{(t+1)} = \pi^{\mathcal{E}}_{(t)} \cup \left(e_i^{\mathrm{A}}, e_j^{\mathrm{B}}\right)$ is given. A pair of non-terminal matched edges is selected from the current matching set $(e_u^{\mathrm{A}}, e_v^{\mathrm{B}}) \in \pi^{\mathcal{E}}_{(t)}$. Let the end-vertices of e_u^{A} and e_v^{B} be the start-vertices of newly matched edges e_i^{A} and e_j^{B}. Then, traverse the end-vertices of e_i^{A} and e_j^{B} in a certain range along the vessel topology. This range is determined by defining the super-edges [13], that is, the path composed of K consecutive edges, K equals 2 or 3 in this paper. Besides, the newly matched edges e_i^{A} and e_j^{B} should not overlap with the edges of $\pi^{\mathcal{E}}_{(t)}$. Therefore, given the current edge matching $\pi^{\mathcal{E}}_{(t)}$, we can obtain multiple-candidate matched edges $\left\{\left(e_{i_1}^{\mathrm{A}}, e_{j_1}^{\mathrm{B}}\right), \left(e_{i_2}^{\mathrm{A}}, e_{j_2}^{\mathrm{B}}\right), \ldots, \left(e_{j_k}^{\mathrm{A}}, e_{j_k}^{\mathrm{B}}\right)\right\}$ through the process mentioned above, also known as feasible pairing detection.

A search tree can be constructed in accordance with the continuous states of edge matching. Thus, $\Omega_{\pi^{\mathcal{E}}}$ can be denoted by the search tree. The optimal $\pi^{\mathcal{E}}$ can be obtained by searching the tree. Here, we design an evaluation score with registration Q:

$$Q = \frac{1}{|\mathrm{C}^{\mathrm{A}}|}\sum_i e^{-\left(\min\limits_j \left\|P\circ T(c_i^{\mathrm{A}}) - c_j^{\mathrm{B}}\right\|\right)/\sigma} + e^{-\left(\frac{s^{\mathrm{A}}}{s^{\mathrm{B}}} + \frac{s^{\mathrm{B}}}{s^{\mathrm{A}}} - 2\right)}. \quad (2)$$

For a given $\pi^{\mathcal{E}}$, the transformation can be estimated through the two surjections $T = f_1\left(f_2(\pi^{\mathcal{E}})\right)$. The first item of the score is associated with the overlapping degree. The minimal distance between the projected 3D point $P \circ T\left(\boldsymbol{c}_i^{\mathrm{A}}\right)$ and 2D point $\boldsymbol{c}_j^{\mathrm{B}}$ can be computed using distance transform, and σ is the scale parameter to normalize the distance. The second item is employed to penalize the scaling in 3D-to-2D projection. s^{A} and s^{B} denote the distribution scales of projected 3D vertex points $\mathcal{V}^{\mathrm{A}}$ and 2D vertex points $\mathcal{V}^{\mathrm{B}}$, respectively. Let matrix $\mathbf{A} \in \mathbb{R}^{|\mathcal{V}^{\mathrm{A}}|\times d}$ denote points of $P \circ T(\mathcal{V}^{\mathrm{A}})$, and matrix $\mathbf{B} \in \mathbb{R}^{|\mathcal{V}^{\mathrm{B}}|\times d}$ denote points of $\mathcal{V}^{\mathrm{B}}$, then $s^{\mathrm{A}} = \det(\mathbf{A}^T\mathbf{A}/|\mathcal{V}^{\mathrm{A}}|)^{\frac{1}{2d}}$ and $s^{\mathrm{B}} = \det(\mathbf{B}^T\mathbf{B}/|\mathcal{V}^{\mathrm{B}}|)^{\frac{1}{2d}}$, $d = 2$. Thus, Q ranges from 0 to 2.

We adopt a variant of the Monte Carlo tree search [15] in this study. The score defined in Eq. (2) is taken as the reward of each node. The purpose of MCTS is to find a node with the highest reward in the domain $\Omega_{\pi^{\mathcal{E}}}$ in which the critical step is accurately selecting the child nodes of the current state. This is achieved by iteratively building a partial search tree, as illustrated in Fig. 1. MCTS extends a partial search tree iteratively by performing the following steps:

Selection: Select the most urgent expandable node in the current tree, which can be achieved by a top-down greedy strategy in each layer starting from the root node. A node is expandable means that at least a new pair of matching edges can be found based on the matching state of the current node. The urgency of node is calculated as follows,

$$Q_u = Q_{sim} + \gamma\sqrt{\frac{2\log N}{n}}, \quad (3)$$

where Q_{sim} is associated with the possible max reward of subtree root in current node, it is calculated in simulation step. N denotes the iteration counts, n denotes the visit times of current node. Thus, the second item is used to penalize the visit times to encourage exploration of un-visited branch. γ is adopted to balance the exploitation of known good nodes and exploration of unvisited nodes.

Expansion: For the selected node, add at most N_{exp} child nodes into the partial search tree. When $> N_{exp}$ child nodes exist, we calculate reward Q for each node and select N_{exp} child nodes with the higher reward.

Simulation: Take each expanded node as root and visit the nodes downward in a depth-first manner. At each layer, we randomly select the child nodes until the deepest leaf node is reached. The process is repeated N_{sim} times, and then the rewards of these visited leaf nodes are calculated. Take the highest reward as the Q_{sim} of the expanded node.

Backpropagation: Update Q_{sim} and the visit times n

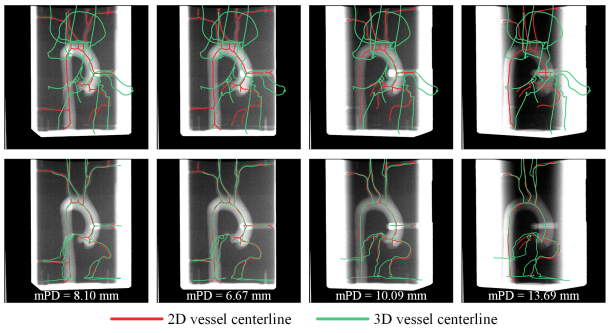

Fig. 2. Results of aorta model experiments. Projected 3D and 2D centerlines are shown in green and red, respectively. The vessels of the initial state are presented in the first row. Results of MCTSR are presented in the second. Frames of Nos. 1, 7, 13, and 19 are shown from left to right.

along the path from the selected node back to the root node.

These four steps are iterated until a computational budget N_{max} is reached or the theoretical maximum reward Q_{max} is obtained. After the iteration, the node with the maximum reward Q value is obtained from the built partial search tree, and its corresponding $\pi^{\mathcal{E}}$ and transformation T are the final results of this method.

III. Experimental Results

3.1 Dataset and Implementation Details

The experiments in this study are performed on aorta model and clinical coronary arteries data. The aorta model corresponds to the normal aortic arch with the left and right coronary arteries (*www.elastrat.com*). The size of the model is 26 cm × 17 cm × 14 cm. A Siemens SOMATOM Definition Flash CT is used to scan the model and derives the corresponding volume data. A rotational C-arm device is similarly used to produce rotational X-ray images. One image frame is captured when the C-arm rotates 2.5°, and a total of 20 frames is acquired. The coronary artery dataset consists of intra-patient CTA and XRA coronary images from 14 patients in Peking Union Medical College Hospital. A total of 54 pairs of 3D and 2D vessel data are used, comprising 22 pairs of right coronary arteries (RCA) and 32 pairs of left coronary arteries (LCA).

The CTA images of the aorta model and coronary arteries are preprocessed using medical image processing software (*Materialise Mimics*). The 3D centerlines and connectivity of vessel branches can be acquired from the software outputs. The X-ray images of the aorta model are segmented manually, whereas the XRA images of the coronary arteries are segmented using a convolutional neural network based method. Then the 2D centerlines are extracted through image thinning. The 2D graphs can be obtained on the basis of neighbor relations.

The 3D/2D registration is evaluated by calculating the mean projected distance (mPD) [16] between projected 3D and 2D centerline points. The performance of the proposed 3D/2D registration method is compared with four comparative methods: 1) An extension of ICP (i.e., ICP-BP) to the 3D/2D application [3], 2) an accelerated method for ICP matching (i.e., DT) [5] by using a precomputed distance transform of 2D vessel centerlines, 3) tree topology matching for 3D/2D registration (i.e., Tree) using tree topology

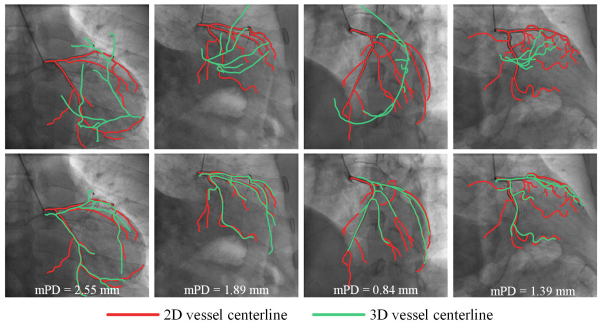

Fig. 3. Results of 3D/2D registration conducted on LCA data. The vessels of the initial state are presented in the first row. Results of MCTSR are presented in the second row.

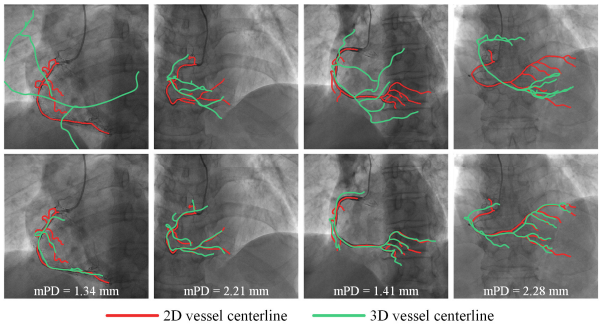

Fig. 4. Results of 3D/2D registration conducted on RCA data. The vessels of the initial state are presented in the first row. Results of MCTSR are presented in the second row.

consistency [17], and 4) OGMM [4]. The parameters of MCTSR are selected empirically. We set the node score parameter $\sigma = 5$, $\gamma = 0.001$, $N_{exp} = 2$, $N_{sim} = 10$, $Q_{max} = 1.8$, and $N_{max} = 200$.

3.2 Experiments and Discussion

Initial vertex pairings for aorta graphs are manually labeled. The 3D aorta graph is registered to 20 frames of the 2D graph. The results of the aorta model experiment are visualized by centerlines, as presented in Figs. 2. The *1st, 7th, 13rd, and 19th* frames are selected for display from left to right. The first row indicates the initial pose of the projected 3D and 2D vessels. The second and third rows indicate the MCTSR results. The results in Fig. 2 present a good overlap of 3D and 2D vessels. The errors are computed using the mPD (unit: mm). The MCTSR achieves an average accuracy of 9.34 mm, which is tolerable with respect to the size of the aorta model. The four comparative methods, ICP-BP, DT, Tree, and OGMM, achieve average accuracies of 15.91, 15.94, 21.48, and 19.91 mm, respectively.

The initial vertex pairings for coronary graphs are automatically recognized by selecting the vertex with the maximum radius. The translation between 3D and 2D data is adjusted by an automatic normalization operation, whereas the rotations are retained. Samples of 3D/2D registration performed on LCA and RCA data are respectively presented in Figs. 3 and 4 in the form of 3D centerlines overlapping the X-ray images. Projected 3D and 2D centerlines are shown respectively in green and red. The distance errors are presented below the respective plotted sub-figures. The MCTSR achieves an average accuracy of 1.91 mm, and the four comparative methods (ICP-BP, DT, Tree, and OGMM)

achieve average accuracies of 4.01, 4.70, 6.51, and 5.15 mm, respectively.

Furthermore, we also record the computation times of all the methods on coronary artery data. The codes are processed on a PC (Intel I7-7700 CPU, MATLAB platform). DT precomputes a distance transform of the 2D centerline; thus, it performs the fastest among all the methods. Detailed statistical results of all methods are presented in Table I.

Table I. Statistical results of all methods

	Aorta model data		Clinical coronary arteries	
	Distance error (mm)	Running time (s)	Distance error (mm)	Running time (s)
ICP-BP	15.91(±0.81)	0.76(±0.02)	4.01(±2.13)	0.45(±0.09)
DT	15.94(±0.80)	0.07(±0.03)	4.70(±2.56)	0.06(±0.01)
Tree	21.48(±4.06)	13.61(±1.69)	6.51(±3.23)	13.21(±5.48)
OGMM	19.91(±3.31)	11.21(±4.25)	5.15(±3.27)	10.39(±5.21)
MCTSR	9.34(±2.66)	9.98(±2.21)	1.91(±0.85)	10.66(±2.76)

IV. Conclusion

In this study, a Monte Carlo tree search based 3D/2D vessel graphs registration method (MCTSR) is proposed. Based on the vessel topology, this work transfers the registration problem to a tree search problem. Then, the Monte Carlo tree search is applied to find the optimal vessel matching result associated with high the registration score. Given that matching only relies on the topology information of 3D and 2D vessels, the proposed method is insensitive to the initial pose.

The experiment results demonstrate that the proposed method is barely sensitive to the initial pose, even with noise disturbance and deformation. Although the translation between 3D and 2D data is adjusted automatically for pose initialization-dependent methods, these methods result in false registration in most cases. The proposed method aims to find matching and then calculate the transformation based on the topological consistency and dense matching of vessel points. Thus, the MCTSR can align un-initialized data. Besides, the MCTSR is time consuming for the large search space of the Monte Carlo search tree. Therefore, it is suitable for the initial pose alignment of 3D and 2D vessels in clinical practice.

Acknowledgement

This work was supported by the National Key R&D Program of China (2017YFC0112000), National Science and Technology Major Project of China (2018ZX10723-204-008) and the National Science Foundation Program of China (81627803, 61501030, 61672099 and 61771056)

References

[1] P. Markelj, D. Tomaževič, B. Likar, and F. Pernuš, "A review of 3D/2D registration methods for image-guided interventions," *Medical Image Analysis,* vol. 16, no. 3, pp. 642-661, 2012/04/01/ 2012.

[2] B. Maiseli, Y. Gu, and H. Gao, "Recent developments and trends in point set registration methods," *Journal of Visual Communication and Image Representation,* vol. 46, pp. 95-106, 2017.

[3] P. J. Besl and N. D. McKay, "A method for registration of 3-D shapes," *IEEE Transactions on Pattern Analysis and Machine Intelligence,* vol. 14, no. 2, pp. 239-256, 1992.

[4] N. Baka, C. T. Metz, C. J. Schultz, R. v. Geuns, W. J. Niessen, and T. v. Walsum, "Oriented Gaussian Mixture Models for Nonrigid 2D/3D Coronary Artery Registration," *IEEE Transactions on Medical Imaging,* vol. 33, no. 5, pp. 1023-1034, 2014.

[5] D. Rivest-Henault, H. Sundar, and M. Cheriet, "Nonrigid 2D/3D registration of coronary artery models with live fluoroscopy for guidance of cardiac interventions," *IEEE Transactions on Medical Imaging,* vol. 31, no. 8, pp. 1557-1572, 2012.

[6] T. Benseghir, G. Malandain, and R. Vaillant, "Iterative closest curve: a framework for curvilinear structure registration application to 2d/3d coronary arteries registration," in *International Conference on Medical Image Computing and Computer-Assisted Intervention*, 2013: Springer, pp. 179-186.

[7] A. Myronenko and X. Song, "Point Set Registration: Coherent Point Drift," *IEEE Transactions on Pattern Analysis and Machine Intelligence,* vol. 32, no. 12, pp. 2262-2275, 2010.

[8] X. Kang *et al.*, "Robustness and accuracy of feature-based single image 2-d–3-d registration without correspondences for image-guided intervention," *IEEE Transactions on Biomedical Engineering,* vol. 61, no. 1, pp. 149-161, 2013.

[9] B. Jian and B. C. Vemuri, "Robust Point Set Registration Using Gaussian Mixture Models," *IEEE Transactions on Pattern Analysis and Machine Intelligence,* vol. 33, no. 8, pp. 1633-1645, 2011.

[10] J. Fan, J. Yang, F. Lu, D. Ai, Y. Zhao, and Y. Wang, "3-Points Convex Hull Matching (3PCHM) for fast and robust point set registration," *Neurocomputing,* vol. 194, pp. 227-240, 2016.

[11] J. Fan *et al.*, "Convex hull indexed Gaussian mixture model (CH-GMM) for 3D point set registration," *Pattern Recognition,* vol. 59, pp. 126-141, 2016.

[12] E. Serradell, M. A. Pinheiro, R. Sznitman, J. Kybic, F. Moreno-Noguer, and P. Fua, "Non-rigid graph registration using active testing search," *IEEE Transactions on Pattern Analysis and Machine Intelligence,* vol. 37, no. 3, pp. 625-638, 2014.

[13] M. A. Pinheiro, J. Kybic, and P. Fua, "Geometric graph matching using monte carlo tree search," *IEEE Transactions on Pattern Analysis and Machine Intelligence,* vol. 39, no. 11, pp. 2171-2185, 2016.

[14] L. Ferraz, X. Binefa, and F. Moreno-Noguer, "Very Fast Solution to the PnP Problem with Algebraic Outlier Rejection," in *2014 IEEE Conference on Computer Vision and Pattern Recognition*, 2014, pp. 501-508.

[15] C. B. Browne *et al.*, "A Survey of Monte Carlo Tree Search Methods," *IEEE Transactions on Computational Intelligence and AI in Games,* vol. 4, no. 1, pp. 1-43, 2012.

[16] E. B. v. d. Kraats, G. P. Penney, D. Tomazevic, T. v. Walsum, and W. J. Niessen, "Standardized evaluation methodology for 2-D-3-D registration," *IEEE Transactions on Medical Imaging,* vol. 24, no. 9, pp. 1177-1189, 2005.

[17] T. Benseghir, G. Malandain, and R. Vaillant, "A tree-topology preserving pairing for 3D/2D registration," *International Journal of Computer Assisted Radiology and Surgery,* vol. 10, no. 6, pp. 913-923, 2015/06/01 2015.